Int J Thermophys (2008) 29:1278–1298
DOI 10.1007/s10765-008-0469-y

A Two-Dimensional Analytical Solution for the Transient Short-Hot-Wire Method

P. L. Woodfield · J. Fukai · M. Fujii · Y. Takata · K. Shinzato

Received: 26 December 2007 / Accepted: 6 June 2008 / Published online: 27 June 2008

Abstract Unlike the conventional transient hot-wire method for measuring thermal conductivity, the transient short-hot-wire method uses only one short thermal-conductivity cell. Until now, this method has depended on numerical solutions of the two-dimensional unsteady heat conduction equation to account for end effects. In order to provide an alternative and to confirm the validity of the numerical solutions, a two-dimensional analytical solution for unsteady-state heat conduction is derived using Laplace and finite Fourier transforms. An isothermal boundary condition is assumed for the end of the cell, where the hot wire connects to the supporting leads. The radial temperature gradient in the wire is neglected. A high-resolution finite-volume numerical solution is found to be in excellent agreement with the present analytical solution.

Keywords Analytical solution · Thermal-conductivity measurement · Transient short hot wire

Nomenclature

a Thermal diffusivity of sample
a_w Thermal diffusivity of wire

P. L. Woodfield (✉) · M. Fujii · K. Shinzato
Research Center for Hydrogen Industrial Use and Storage, National Institute of Advanced Industrial Science and Technology, 744 Mootoka, Nishi-ku, Fukuoka 819-0395, Japan
e-mail: p.woodfield@aist.go.jp

J. Fukai
Department of Chemical Engineering, Graduate School of Engineering, Kyushu University, Nishi-ku, Fukuoka 819-0395, Japan

Y. Takata
Department of Mechanical Engineering Science, Kyushu University, Nishi-ku, Fukuoka 819-0395, Japan

b_n Constant specified after Eq. 11
i Square root of -1
I_0 0th-Order modified Bessel function of the first kind
I_1 1st-Order modified Bessel function of the first kind
J_0 0th-Order Bessel function of the first kind
J_1 1st-Order Bessel function of the first kind
K_0 0th-Order modified Bessel function of the second kind
K_1 1st-Order modified Bessel function of the second kind
L Half the length of the wire
m_n nth Eigenvalue (Eq. 10)
q Heat supplied per unit time per unit length of wire
Q Heat supplied to wire per unit time per unit volume
r Radial coordinate
r_0 Radius of wire
R Radius of hot-wire cell
s Laplace transform parameter
t Time
T Temperature rise in the sample from the initial condition
T_w Temperature rise in the wire from the initial condition
Y_0 0th-Order Bessel function of the second kind
Y_1 1st-Order Bessel function of the second kind
z Axial coordinate

Greek

α_n Root of Eq. 13
β Constant specified after Eq. 11
Δ' Function given by Eq. 14
λ Thermal conductivity
λ_w Thermal conductivity of wire
Λ' Function given by Eq. 18
ϕ_n Root of Eq. 17
θ_n Unsteady part of the solution for the nth eigenvalue
Θ_n Steady part of the solution for the nth eigenvalue
ζ_n Function given by Eq. 16

1 Introduction

The transient short-hot-wire method for measuring thermal conductivity and thermal diffusivity was developed in the late 1990s by Fujii et al. [1–3]. It is a variant of the conventional transient hot-wire method with the novelty that only one short conductivity cell is used and end effects are accounted for by numerical simulation of unsteady heat conduction in the cell. The method is particularly useful for corrosive or electrically conductive fluids, where it is necessary to apply protective coatings to the wire [3]. For such applications, short wire reduces the probability of failure of the insulation.

Another important potential application is the study of high-pressure gas thermal conductivity [4], where a small-volume pressure vessel is highly desirable, particularly from the point of view of ease of conformity with high-pressure gas regulations.

Recently the transient short-hot-wire method was extended by the present authors [5] to make it applicable to low-density gases and conditions, where the temperature rise is no longer a linear function of the logarithm of time. An algorithm was developed based on the Gauss–Newton nonlinear least-squares method to simultaneously determine thermal conductivity and thermal diffusivity. However, an underlying concern with any property measurement technique that makes use of numerical solutions is that it is necessary to guarantee that numerical errors have been reduced to at least an order of magnitude smaller than the experimental error. If this is not possible, then the numerical error must be included in the uncertainty estimation for the fluid property. Woodfield et al. [5] demonstrated numerical grid convergence and made estimates of the numerical error using progressively finer grid spacing. This is an important test, but to obtain an absolute estimate of the numerical error, it is desirable to compare numerical solutions with exact analytical solutions.

Assael et al. [6] compared their one-dimensional finite element solution for the transient hot-wire method with the well-known asymptotic one-dimensional analytical solution applicable for large time in an infinite medium. Fujii et al. [1] also made use of the one-dimensional analytical solution to estimate the absolute numerical error in their method based on the limiting case of a long wire. While the one-dimensional asymptotic case is a useful test, it would be much better if two-dimensional analytical solutions were available to check the accuracy at conditions, where end effects are important. This is especially true for the short-hot-wire method since the instrument usually operates at conditions, where the effect of the finite length is large. Thus, the primary purpose of the present article is to provide a two-dimensional analytical solution for validation of numerical solutions used in the short-hot-wire method. If the hot-wire cell is designed such that the boundary conditions for the present analytical solution are valid, then it is recommended that the analytical solution be used directly in place of the numerical solution.

In 1976, Healy et al. [7] observed concerning the finite length of the wire that at that time it was "not possible to account for such end effects analytically" (p. 394). For this reason, experimental approaches, such as that using two wires of differing lengths are usually applied to compensate for end effects [8]. However, a few years prior to the publication of Ref. [7] a solution to the two-dimensional problem had already been derived analytically by Kierkus et al. [9] assuming isothermal boundaries at the ends and an infinite boundary in the radial direction. Moreover, for isothermal boundaries, the two-dimensional steady-state case was solved as early as the 1930s by Kannuluik and Martin [10,11] to correct for end effects in a steady-state hot-wire cell. In a sense the above mentioned statement from Healy et al. [7] is still correct since analytically, a complete treatment of the end effects may be extremely difficult, if not impossible, due to the complicated geometry of the wire supports. However, for some cases the end effects may be well approximated by an isothermal boundary [1,2]. The reason for this is that it takes time for the heating effect from the wire to extend beyond a local region surrounding the attachment point of the hot wire to its support which itself has a large thermal inertia. For high thermal-diffusivity fluids

(i.e., low-density gases) however, we must revert to numerical solutions for the transient short-hot-wire method since the effect of the support geometry starts to become important [5].

The present article extends the work of Kierkus et al. [9] by deriving the solution for the case of a finite-diameter cell. The technique itself for deriving the present solution is not new, but we believe that solving this problem analytically is a useful contribution towards strengthening the foundation of the transient short-hot-wire method. The approach used in the present study is an extension of that used for the one-dimensional unsteady solutions by Carslaw and Jaeger for a finite hollow cylinder (Sect. 13.4 in Ref. [12] and Refs. [13] and [14] for more general boundary conditions for the 1D case).

2 Analytical Solution

2.1 Domain and Boundary Conditions

Figure 1 shows the domain and boundary conditions for the problem under consideration. T denotes the rise in temperature from the initial condition, and the wire has a length of $2L$. For the wire, neglecting the radial temperature gradient ($r \leq r_0$),

$$\frac{1}{a_w}\frac{\partial T_w}{\partial t} = \frac{\partial^2 T_w}{\partial z^2} + \frac{Q}{\lambda_w} + \frac{2\lambda}{r_0 \lambda_w}\frac{\partial T}{\partial r}\Big|_{r=r_0} \tag{1}$$

$$Q = q/\pi r_0^2 \tag{1a}$$

The subscript w refers to the wire properties and temperatures, and no subscript refers to the gas sample. The second term on the right-hand side of Eq. 1 represents Joule

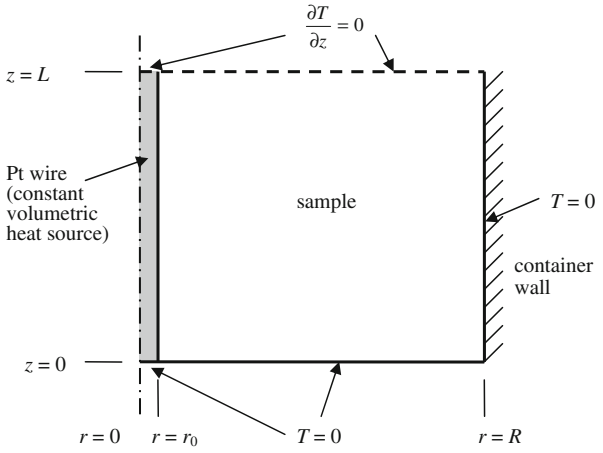

Fig. 1 Domain and boundary conditions for analytical solution

heating, which is assumed to be constant for $t > 0$, and the third term on the right-hand side arises due to heat conduction into the sample. Note that neglecting the radial temperature gradient in the wire greatly simplifies the analytical problem. The justification for this assumption is discussed later in this article.

For the gas ($r \geq r_0$), unsteady heat conduction is given by

$$\frac{1}{a}\frac{\partial T}{\partial t} = \frac{1}{r}\frac{\partial}{\partial r}\left(r\frac{\partial T}{\partial r}\right) + \frac{\partial^2 T}{\partial z^2} \tag{2}$$

The boundary and initial conditions are given by

$$T|_{r=R} = 0 \tag{3}$$

$$T|_{z=0} = T_{\mathrm{w}}|_{z=0} = 0 \tag{4}$$

$$\frac{\partial T_{\mathrm{w}}}{\partial z}|_{z=L} = \frac{\partial T}{\partial z}|_{z=L} = 0 \tag{5}$$

$$T_{\mathrm{w}} = T|_{r=r_0} \tag{6}$$

$$T|_{t=0} = T_{\mathrm{w}}|_{t=0} = 0 \tag{7}$$

2.2 Analytical Solution Technique

Equations 1–7 were solved analytically using the Laplace and finite Fourier transforms as follows: Laplace transform → finite Fourier transform → solve the one-dimensional ordinary differential equation → inverse Laplace transform (residue method) → inverse Fourier transform → final solution. Details of the derivation are given in Appendix A.

2.3 Final Solution

The temperature rise at any time and point (t, r, z) in the sample is given by

$$T\,(r, z, t) = \sqrt{\frac{2}{L}}\sum_{n=1}^{\infty}\sin\,(m_n z)\,(\Theta_n\,(r) + \theta_n\,(r, t)) \quad r_0 \leq r \leq R, 0 \leq z \leq L \tag{8}$$

Integrating Eq. 8 from $z = 0$ to $z = L$, dividing by L, and setting $r = r_0$ gives the volume-averaged temperature rise in the wire as

$$T_{\mathrm{w(av)}}\,(t) = \sqrt{\frac{2}{L^3}}\sum_{n=1}^{\infty}\frac{1}{m_n}\,(\Theta_n\,(r_0) + \theta_n\,(r_0, t)) \tag{9}$$

Note that $\cos(m_n L) = 0$ for all m_n. In Eq. 9, L is half the length of the wire and the eigenvalues are given by

$$m_n = \frac{2n-1}{L}\frac{\pi}{2} \tag{10}$$

The steady part of the solution is given as

$$\begin{aligned}\Theta_n(r) = b_n\,(&-K_0(m_nR)\,I_0(m_nr)\\ &+ I_0(m_nR)\,K_0(m_nr))\,/\left(I_0(m_nR)\left(m_n^2K_0(m_nr_0)+\beta m_nK_1(m_nr_0)\right)\right.\\ &\left.- K_0(m_nR)\left(m_n^2I_0(m_nr_0)-\beta m_nI_1(m_nr_0)\right)\right)\end{aligned} \tag{11}$$

The functions K_0, I_0, I_1, and K_1 are modified Bessel functions and β and b_n are given by

$$\beta = \frac{2\lambda}{r_0\lambda_w} \quad b_n = \sqrt{\frac{2}{L}}\frac{Q}{m_n\lambda_w}$$

The transient part of the solution used in Eqs. 8 and 9 is given by

$$\begin{aligned}\theta_n(r,t) = \zeta_n(\phi_n)\\ +\sum_{j=1}^{\infty}\frac{b_n\pi}{2}\frac{J_0(\alpha_{j,n}R)\,Y_0(\alpha_{j,n}r)-Y_0(\alpha_{j,n}R)\,J_0(\alpha_{j,n}r)}{-a\left(\alpha_{j,n}^2+m_n^2\right)\Delta'(\alpha_{j,n})}e^{-a\left(\alpha_{j,n}^2+m_n^2\right)t}\end{aligned} \tag{12}$$

where J_0 and Y_0 are Bessel functions of the first and second kinds, respectively.

The constant, $\alpha_{j,n}$, is the jth positive real root of

$$\begin{aligned}J_0(\alpha_nR)\left(\left(\frac{-a\left(\alpha_n^2+m_n^2\right)}{a_w}+m_n^2\right)Y_0(\alpha_nr_0)+\beta\alpha_nY_1(\alpha_nr_0)\right)\\ -Y_0(\alpha_nR)\left(\left(\frac{-a\left(\alpha_n^2+m_n^2\right)}{a_w}+m_n^2\right)J_0(\alpha_nr_0)+\beta\alpha_nJ_1(\alpha_nr_0)\right)=0\end{aligned} \tag{13}$$

The function Δ' in the denominator of Eq. 12 is given as

$$\begin{aligned}\Delta'(\alpha_n) = \frac{-\pi}{4a\alpha_n}\{&-RJ_1(\alpha_nR)\,[A_nY_0(\alpha_nr_0)+\beta\alpha_nY_1(\alpha_nr_0)]\\ &+J_0(\alpha_nR)\,[(\beta\alpha_nr_0-2\alpha_n(a/a_w))\,Y_0(\alpha_nr_0)-A_nr_0Y_1(\alpha_nr_0)]\\ &+RY_1(\alpha_nR)\,[A_nJ_0(\alpha_nr_0)+\beta\alpha_nJ_1(\alpha_nr_0)]\\ &-Y_0(\alpha_nR)\,[(\beta\alpha_nr_0-2\alpha_n(a/a_w))\,J_0(\alpha_nr_0)-A_nr_0J_1(\alpha_nr_0)]\}\end{aligned} \tag{14}$$

J_1 and Y_1 are first-order Bessel functions of the first and second kinds, respectively. The parameter A_n is given by

$$A_n = \frac{-a\left(\alpha_n^2 + m_n^2\right)}{a_w} + m_n^2$$

The first term on the right-hand side of Eq. 12, $\zeta_n(\phi)$, appears if Eq. 13 has complex roots. The complex roots only appear if the thermal diffusivity of the gas is larger than the thermal diffusivity of the wire, and even then only at sufficiently large values of m. If either of the conditions given in Eq. 15 are satisfied, $\zeta_n(\phi)$ is zero. Proof of this is given in Appendix B.

$$\zeta(\phi) = 0 \text{ when } \quad a \le a_w \quad \text{or} \quad m_n^2 < \beta/\{((a/a_w) - 1)\, r_0 \ln(R/r_0)\} \tag{15}$$

If both of the conditions in Eq. 15 are not satisfied, then $\zeta_n(\phi)$ is given by

$$\zeta_n(\phi_n) = \frac{b}{a\left(\phi_n^2 - m_n^2\right)\Lambda'(\phi_n)} \left(K_0(\phi_n R)\, I_0(\phi_n r) - I_0(\phi_n R)\, K_0(\phi_n r)\right) e^{-a\left(m_n^2 - \phi_n^2\right)t}$$
$$\text{when } a > a_w \text{ and } m_n^2 > \beta/\{((a/a_w) - 1)\, r_0 \ln(R/r_0)\} \tag{16}$$

ϕ_n is the positive real root of

$$\left(I_0(\phi_n R)\, K_0(\phi_n r_0) - K_0(\phi_n R)\, I_0(\phi_n r_0)\right)\left(\left(\phi_n^2 - m_n^2\right)(a/a_w) + m_n^2\right)$$
$$+ \left(I_0(\phi_n R)\, K_1(\phi_n r_0) + K_0(\phi_n R)\, I_1(\phi_n r_0)\right)\beta\phi_n = 0 \tag{17}$$

The function in the denominator of Eq. 16, $\Lambda'(\phi_n)$, is given by

$$\Lambda'(\phi_n) = \frac{1}{2\phi_n a}\left[\left(K_0(\phi_n R)\, I_0(\phi_n r_0) - I_0(\phi_n R)\, K_0(\phi_n r_0)\right)\left(2(a/a_w) - \beta r_0\right)\phi_n\right.$$
$$+ \left(r_0 K_0(\phi_n R)\, I_1(\phi_n r_0) - R K_1(\phi_n R)\, I_0(\phi_n r_0)\right) B_n$$
$$+ \left(r_0 I_0(\phi_n R)\, K_1(\phi_n r_0) - R I_1(\phi_n R)\, K_0(\phi_n r_0)\right) B_n$$
$$\left. + \left(K_1(\phi_n R)\, I_1(\phi_n r_0) - I_1(\phi_n R)\, K_1(\phi_n r_0)\right)\beta\phi_n R\right] \tag{18}$$

where

$$B_n = m_n^2 + \frac{\left(\phi_n^2 - m_n^2\right)a}{a_w}$$

For ease of computation, note that for Eq. 17 the positive real root lies in the range given by Eq. 19. This can be deduced from Eq. 17 as explained in Appendix B;

$$0 < \phi_n^2 < m_n^2\left(1 - (a_w/a)\right) \tag{19}$$

Notice that the transient term (Eq. 12) tends to zero for large t so that in the steady-state only Eq. 11 is needed for evaluation of Eq. 8. Moreover, Eq. 12 will converge quickly

if t is large, implying that fewer terms will be required as the solution approaches the steady state. Unfortunately the modified Bessel functions required for Eqs. 11 and 16–18 do not usually come as standard with FORTRAN compilers so for the present study the expansions given in Ref. [15] were used. Perhaps the most tedious part of implementing the above analytical solution is finding the roots of Eq. 13. This can be done in a computer program by observing that the roots are spaced at a distance of approximately π/R apart. Once an approximate location of the root is known, accurate evaluation can be done using a numerical search procedure such as the Newton–Raphson method or the bisection method.

3 Comparison with Finite-Volume Numerical Solution

As mentioned above, the main purpose for deriving the present analytical solution is an estimation of the absolute error in the numerical solution for the transient short-hot-wire method. Therefore, as an example, we take the case of hydrogen gas at atmospheric pressure and 25 °C as was also considered in Ref. [5]. The mathematical model used in the finite-volume numerical solution is the same as that specified in Eqs. 1– 7 except that the radial temperature gradient in the wire neglected in Eq. 1 was included in the numerical solution. Details of the problem geometry, conditions, and assumed thermal properties are listed in Table 1. Full details of the numerical grid and procedure for the finite-volume solution are also given in Ref. [5].

Figure 2 gives a comparison of the present analytical solution with the finite-volume numerical solution. The temperature rise is the volume-averaged temperature rise in the wire as specified in Eq. 9. The agreement is excellent, and the two cases are indistinguishable in the figure. Table 2 gives a comparison of specific points using two different numerical grid arrangements.

We can see from Table 2 that the finer grid ($N_r \times N_z = 600 \times 75$) is closer to the analytical solution than the 300×38 grid, as should be expected. The largest error is at the smallest value of time ($t = 0.02$ s) but it is still less than 0.1 % (about 1 mK) even for the 300×38 grid. Table 2 confirms that the high resolution numerical solution in Ref. [5] is reliable, and thus, is suitable for evaluation of thermal conductivity. Moreover, the analytical solution given in Table 2 may be considered as bench-mark quality data for testing of numerical codes developed for the transient short-hot-wire method.

Table 1 Test problem specifications (hydrogen gas at atmospheric pressure, 25 °C)

q(W·m^{-1})	Gas		Platinum wire		r_0 (μm)	R(mm)	L(mm)
	a (10^{-4}m^2·s^{-1})	λ (W·m^{-1}·K^{-1})	a_w (10^{-5}m^2·s^{-1})	λ_w (W·m^{-1}·K^{-1})			
0.295	1.57	0.185	2.51	71.6	5	10	10

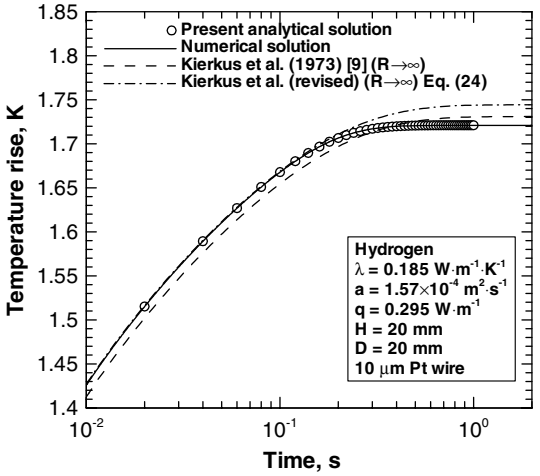

Fig. 2 Comparison with numerical solution for volume-averaged wire temperature rise

Table 2 Comparison of analytical and numerical calculations for temperature rise

Time (s)	Analytical T (K)	Numerical 600 × 75 grid		Numerical 300 × 38 grid	
		T (K)	Error (%)	T (K)	Error (%)
0.02	1.51533	1.51515	0.012	1.51426	0.071
0.06	1.62706	1.62691	0.009	1.62607	0.061
0.10	1.66790	1.66775	0.009	1.66691	0.059
0.14	1.68975	1.68960	0.009	1.68875	0.059
0.18	1.70245	1.70230	0.009	1.70145	0.059
0.22	1.70998	1.70984	0.008	1.70899	0.058
0.26	1.71447	1.71434	0.008	1.71349	0.057
0.30	1.71715	1.71702	0.007	1.71618	0.057

4 Comparison with Solution by Kierkus et al. [9]

Kierkus et al. [9] derived a solution for the same problem as in the present article except that the boundary condition in Eq. 3 is replaced by

$$T|_{r\to\infty} = 0 \tag{20}$$

In terms of the present notation, their solution for the volume-averaged wire temperature can be written as

$$T_{\mathrm{w(av)}}(t) = \frac{4q}{L^2\pi^2\lambda}\sum_{n=1}^{\infty}\frac{1}{m_n^2}\int_0^{\infty}\frac{\left(1-\mathrm{e}^{-\left(u^2+m_n^2r_0^2\right)at/r_0^2}\right)\left(Y_0(u)\,\phi(u)-J_0(u)\,\psi(u)\right)}{\left(u^2+m_n^2r_0^2\right)\left(\phi^2(u)+\psi^2(u)\right)}u\mathrm{d}u \tag{21}$$

where

$$\varphi(u) = 2uJ_1(u) + \frac{\lambda_w}{\lambda}\left(m_n^2 r_0^2 - \frac{a}{a_w}\left(m_n^2 r_0^2 + u^2\right)\right) J_0(u) \tag{22}$$

$$\psi(u) = 2uY_1(u) + \frac{\lambda_w}{\lambda}\left(m_n^2 r_0^2 - \frac{a}{a_w}\left(m_n^2 r_0^2 + u^2\right)\right) Y_0(u) \tag{23}$$

Note that we have corrected some typographical errors in the result from Ref. [9] and unlike Ref. [9], in the present article L is half of the wire length.

The dashed line in Fig. 2 shows the result of applying Eq. 21 to the case of hydrogen gas at atmospheric pressure. For the boundary condition given in Eq. 20 we should expect the solution by Kierkus et al. [9] to agree with the finite-radius solution at small values of time but then become larger as the effect of the boundary condition at the cell wall becomes important. However, contrary to expectations, the dashed line in Fig. 2 is lower than the finite-domain solutions for values of time less than about 0.2 s. In order to find the reason for this discrepancy, we re-derived the solution of Kierkus et al. and it appears that for reasons of simplicity they may not have included all terms from the inverse Laplace transform. For large values of t, a slightly better (although still not exact) solution is given by

$$T_{w(av)}(t) = T_{wss(av)} - \frac{4q}{L^2\pi^2\lambda}\sum_{n=1}^{\infty}\frac{1}{m_n^2}\int_0^{\infty}\frac{\left(Y_0(u)\,\phi(u) - J_0(u)\,\psi(u)\right)\mathrm{e}^{-\left(u^2+m_n^2r_0^2\right)at/r_0^2}}{\left(u^2+m_n^2r_0^2\right)\left(\phi^2(u)+\psi^2(u)\right)}u\,\mathrm{d}u \tag{24}$$

where the steady-state part of the solution is

$$T_{wss(av)} = \frac{2q}{\pi r_0^2 L^2\lambda}\sum_{n=1}^{\infty}\frac{1}{m_n^3}\frac{K_0(m_n r_0)}{\frac{\lambda_w}{\lambda}m_n K_0(m_n r_0) + \frac{2}{r_0}K_1(m_n r_0)} \tag{25}$$

Equation 24 is also plotted in Fig. 2 as a dashed-dotted line. Consistent with expectations, Eq. 24 is in good agreement with the present analytical solution until time becomes large enough for the cell wall at $r = R$ to have an influence. Note that Eq. 21 may be deduced from Eq. 24 if we assume that Eq. 24 is exact at $t = 0$. However, in deriving Eq. 24, we have neglected a term somewhat analogous to the term $\zeta_n(\phi_n)$ in Eq. 12 that may become important for very small values of t.

5 Convergence of Analytical Solution

Equations 8, 9, and 12 all contain summations to infinity. Therefore, it is useful to confirm that enough terms have been used to obtain an accurate result. In order to do

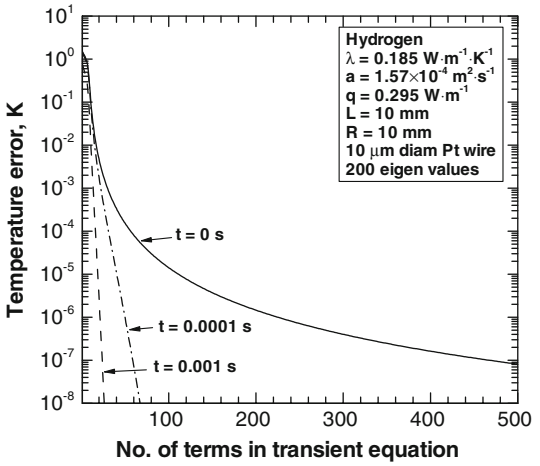

Fig. 3 Convergence of Eq. 9 with respect to the number of terms in Eq. 12

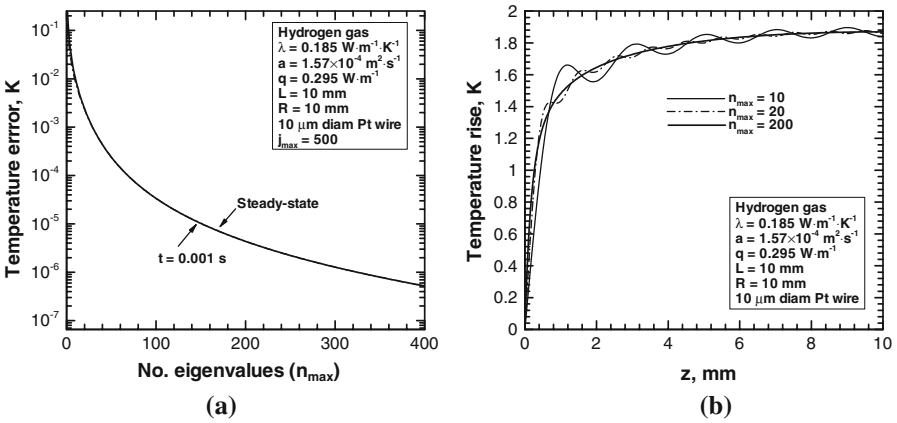

Fig. 4 Convergence of solution with respect to number of eigenvalues: (**a**) error in volume-averaged wire temperature and (**b**) steady-state temperature distribution along wire

this, we will consider the worst case, $t = 0$ and some other cases for small t. For the case $t = 0$, convergence of Eq. 12 will be the slowest since the exponential factor takes on a constant value of unity instead of reducing in size with larger values of j or n. Also, for $t = 0$ the solution is known exactly since it is specified as zero in Eq. 7. Figure 3 shows the error in evaluating Eq. 9 with different numbers of roots $\alpha_{j,n}$ $j = 1$, $j_{\max}$. From Fig. 3 it may be observed that even for the slowest converging case, $t = 0$, the error becomes less than 1 mK by about 50 terms. For practical problems where $t > 0.001$ s, as few as 20 terms may be sufficient.

For the examples shown in Fig. 3, the summation over the eigenvalues $n = 1$ to $n_{\max}$ in Eq. 9 was restricted to $n_{\max} = 200$. Figure 4 shows the effect of changing $n_{\max}$. To calculate the error for Fig. 4a, the 'exact' temperature rise was taken to be the calculated temperature corresponding to 1000 eigenvalues. Figure 4a shows the

Table 3 Volume-averaged wire temperature rise—effect of $\partial T_w/\partial r$

Time (s)	0.02	0.06	0.10	0.14
Temperature (K) with $\partial T_w/\partial r$	1.51515	1.62691	1.66775	1.68960
Temperature (K) without $\partial T_w/\partial r$	1.51503	1.62678	1.66762	1.68946

case for the steady-state and for $t = 0.001$ s. The temperature errors in both cases are almost indistinguishable. This indicates that convergence with respect to the number of eigenvalues is dominated by the steady-state component of the solution (i.e., Eq. 11). Figure 4b shows the calculated temperature distribution along the wire. Quite clearly, using only 10 or 20 eigenfunctions is insufficient to resolve the shape of the temperature distribution. Supposing the experimental error is of the order of millikelvins, then according to Fig. 4a, for a numerical error two orders of magnitude smaller, about 150 eigenvalues should be sufficient. It is worth mentioning here that using more than about 220 eigenvalues that requires quadruple precision to evaluate $\mathrm{I}_0(m_n R)$ in Eq. 11 since the modified Bessel functions of the first kind increase exponentially.

6 Influence of Radial Temperature Gradient in Wire

The present analytical solution would be much more complicated if it were necessary to include the radial temperature gradient in the wire. Therefore, to justify this assumption, we have carried out finite-volume numerical simulations with and without the temperature gradient in the wire. The case considered is the same as that specified in Sect. 3, Table 1. The results for a few selected points in time are shown in Table 3. For this particular example, the difference in the temperature rise due to neglecting the radial temperature gradient in the wire is of the order of 0.1 mK. Since (based on Table 2) the accuracy of the numerical solution is of the same order, a little is achieved by including the radial temperature gradient in the wire in the numerical solution. Notice also in Table 3, that as should be expected, neglecting the radial temperature gradient makes the wire slightly cooler than reality. Of course, the radial temperature gradient in the wire will become more important if the thermal conductivity of the wire is lower.

7 Effect of $\zeta_n(\phi_n)$ in Eq. 12

As mentioned in Sect. 2.3 above, if the thermal diffusivity of the sample fluid is greater than the thermal diffusivity of the wire, then an extra term, $\zeta_n(\phi_n)$, appears in the transient part of the solution (Eq. 12). For a platinum wire, this is only likely to occur in gases at pressures less than about 1 MPa. Since the additional term makes the solution much more complicated, it is worthwhile to test its significance. By inspection of Eq. 16, we can see that $\zeta_n(\phi_n)$ will become less important as t increases. This is confirmed in Fig. 5. Figure 5 shows the calculated temperature rise for the case considered in Sect. 3 with and without $\zeta_n(\phi_n)$.

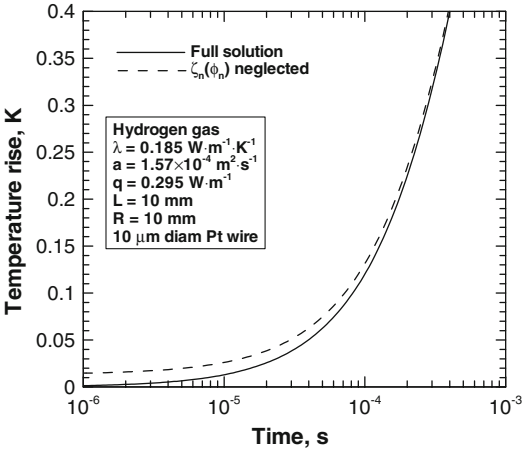

Fig. 5 Effect of neglecting $\zeta_n(\phi_n)$ in Eq. 12

At time zero, the full solution for the case in Fig. 5 is very close to the initial condition, $T = 0$ as is also indicated in Fig. 3. If $\zeta_n(\phi_n)$ is neglected, however, at $t = 0$ the temperature rise has a value of 0.01339 K. At $t = 0.01$ s the difference between the solution including $\zeta_n(\phi_n)$ and the full solution is only 1.5×10^{-7} K. Therefore, for practical purposes, the term $\zeta_n(\phi_n)$ may be neglected without loss of accuracy. Note that the present example of hydrogen at atmospheric pressure is an extreme case. For lower diffusivity fluids, $\zeta_n(\phi_n)$ should be even smaller.

8 Conclusions

The following can be concluded from the present study.

1. The derived analytical solution is a useful tool for validating numerical codes used for the transient short-hot-wire method for measuring thermal conductivity.
2. Bench-mark quality calculated data for a sample high-diffusivity gas case of practical value is given in Table 2.
3. From 100 to 200 eigenvalues should be used in evaluating the summations in Eqs. 8 and 9.
4. The number of terms required for the transient summation, Eq. 12, varies depending on the value of t. For $t > 0.01$ s, fewer than 20 terms should be enough.
5. The term $\zeta_n(\phi_n)$ in Eq. 12 may be neglected for most practical purposes connected with the transient short-hot-wire method.
6. Little accuracy is lost by neglecting the radial temperature gradient in the wire.

Acknowledgments This research has been conducted as a part of the "Fundamental Research Project on Advanced Hydrogen Science" funded by the New Energy and Industrial Technology Development Organization (NEDO).

Appendix A

Derivation of Analytical Solution

Taking Laplace transforms of Eq. 1–6 gives

$$\frac{s}{a_{\mathrm{w}}}\overline{T}_{\mathrm{w}} = \frac{\partial^2 \overline{T}_{\mathrm{w}}}{\partial z^2} + \frac{Q}{s\lambda_{\mathrm{w}}} + \frac{2\lambda}{r_0\lambda_{\mathrm{w}}}\frac{\partial \overline{T}}{\partial r}|_{r=r_0} \tag{A1}$$

$$\frac{s}{a}\overline{T} = \frac{\partial^2 \overline{T}}{\partial z^2} + \frac{1}{r}\frac{\partial}{\partial r}\left(r\frac{\partial \overline{T}}{\partial r}\right) \tag{A2}$$

$$\overline{T}|_{r=R} = 0 \tag{A3}$$

$$\overline{T}_{\mathrm{w}} = \overline{T}|_{r=r_0} \tag{A4}$$

$$\overline{T}_{\mathrm{w}}|_{z=0} = \overline{T}|_{z=0} = 0 \tag{A5}$$

$$\frac{\partial \overline{T}}{\partial z}|_{z=L} = \frac{\partial \overline{T}_{\mathrm{w}}}{\partial z}|_{z=L} = 0 \tag{A6}$$

Next we make use of the following finite Fourier transform (e.g., Ref. [16]);

$$\overline{\overline{f}}\,(m_n) \equiv \sqrt{\frac{2}{L}}\int_0^L \sin(m_n z)\,\bar{f}\,(z)\,\mathrm{d}z \quad m_n = \frac{2n-1}{L}\frac{\pi}{2} \quad n = 1, 2, \ldots \tag{A7}$$

The inverse Fourier transform is given by

$$\bar{f}\,(z) = \sqrt{\frac{2}{L}}\sum_{n=1}^{\infty}\sin(m_n z)\,\overline{\overline{f}}\,(m_n) \tag{A8}$$

Equation A7 is appropriate for satisfying the boundary conditions A5 and A6. Applying Eq. A7 to Eq. A1 through A4, and making use of Eqs. A5 and A6, gives

$$\frac{s}{a_{\mathrm{w}}}\overline{\overline{T_{\mathrm{w}}}} = -m_n^2\overline{\overline{T_{\mathrm{w}}}} + \sqrt{\frac{2}{L}}\frac{Q}{m_n\lambda_{\mathrm{w}}s} + \frac{2\lambda}{r_0\lambda_{\mathrm{w}}}\frac{\mathrm{d}\overline{\overline{T}}}{\mathrm{d}r}|_{r=0} \tag{A9}$$

$$\frac{s}{a}\overline{\overline{T}} = -m_n^2\overline{\overline{T}} + \frac{1}{r}\frac{\mathrm{d}}{\mathrm{d}r}\left(r\frac{\mathrm{d}\overline{\overline{T}}}{\mathrm{d}r}\right) \tag{A10}$$

$$\overline{\overline{T}}|_{r=R} = 0 \tag{A11}$$

$$\overline{\overline{T_{\mathrm{w}}}} = \overline{\overline{T}}|_{r=r_0} \tag{A12}$$

In order to simplify the notation, let $\overline{\theta} = \overline{\overline{T}}$ where θ is the Fourier transform of T and $\overline{\theta}$is the Laplace transform of θ. Substituting Eq. A12 into Eq. A9 and rearranging Eqs. A10 and A11 gives

$$\left(\frac{s}{a_{\mathrm{w}}} + m_n^2\right)\overline{\theta}|_{r=r_0} = \sqrt{\frac{2}{L}}\frac{Q}{m_n\lambda_{\mathrm{w}}s} + \frac{2\lambda}{r_0\lambda_{\mathrm{w}}}\frac{\mathrm{d}\overline{\theta}}{\mathrm{d}r}|_{r=r_0} \tag{A13}$$

$$\left(\frac{s}{a} + m_n^2\right)\overline{\theta} = \frac{1}{r}\frac{\mathrm{d}}{\mathrm{d}r}\left(r\frac{\mathrm{d}\overline{\theta}}{\mathrm{d}r}\right) \tag{A14}$$

$$\overline{\theta}|_{r=R} = 0 \tag{A15}$$

Equation A14 is an ordinary differential equation with boundary conditions expressed by Eqs. A13 and A15. Since Eq. A14 can be rewritten in the form of a modified Bessel equation of order zero by substituting $x = (((s/a) + (m_n)^2)^{1/2}r)$, the general solution is given by Eq. A16, where the constants A and B need to be determined using Eqs. A13 and A15:

$$\overline{\theta} = AI_0\left(\left(\frac{s}{a} + m_n^2\right)^{1/2} r\right) + BK_0\left(\left(\frac{s}{a} + m_n^2\right)^{1/2} r\right) \tag{A16}$$

Solving for A and B gives

$$\begin{aligned}\overline{\theta} = \frac{b_n}{s\Delta}\Bigg(&K_0\left(\left(\frac{s}{a} + m_n^2\right)^{1/2} R\right) I_0\left(\left(\frac{s}{a} + m_n^2\right)^{1/2} r\right)\\ &- I_0\left(\left(\frac{s}{a} + m_n^2\right)^{1/2} R\right) K_0\left(\left(\frac{s}{a} + m_n^2\right)^{1/2} r\right)\Bigg)\end{aligned} \tag{A17}$$

where

$$\begin{aligned}\Delta = &K_0\left(\left(\frac{s}{a} + m_n^2\right)^{1/2} R\right)\Bigg(\left(\frac{s}{a_{\mathrm{w}}} + m_n^2\right) I_0\left(\left(\frac{s}{a} + m_n^2\right)^{1/2} r_0\right)\\ &- \beta\left(\frac{s}{a} + m_n^2\right)^{1/2} I_1\left(\left(\frac{s}{a} + m_n^2\right)^{1/2} r_0\right)\Bigg)\\ &- I_0\left(\left(\frac{s}{a} + m_n^2\right)^{1/2} R\right)\Bigg(\left(\frac{s}{a_{\mathrm{w}}} + m_n^2\right) K_0\left(\left(\frac{s}{a} + m_n^2\right)^{1/2} r_0\right)\\ &+ \beta\left(\frac{s}{a} + m_n^2\right)^{1/2} K_1\left(\left(\frac{s}{a} + m_n^2\right)^{1/2} r_0\right)\Bigg)\end{aligned} \tag{A18}$$

and

$$\beta = \frac{2\lambda}{r_0 \lambda_w} \quad b_n = \sqrt{\frac{2}{L}} \frac{Q}{m_n \lambda_w}$$

In order to find the inverse Laplace transform of Eq. A17, we make use of the inversion formula. For the special case where there is no branch and the integrand tends to zero at infinity (to the left of c on the complex plane), the inverse Laplace transform is given by the sum of the residues as in Eq. A19. Both of these conditions are usually satisfied for heat conduction problems in finite domains;

$$\theta = \frac{1}{2\pi i} \int_{c-i\infty}^{c+i\infty} e^{st} \overline{\theta} ds = \sum \text{residues} \tag{A19}$$

In Eq. A19, c is a positive real constant large enough so that all singularities are to the left of c. Thus, we need to find the singularities in Eq. A17. Poles appear at $s = 0$ and for any values of s that make $\Delta = 0$.

The residue for $s = 0$ is given by

$$\text{res}|_{s=0} = b_n \left(K_0 (m_n R) I_0 (m_n r) - I_0 (m_n R) K_0 (m_n r)\right) / \Big(K_0 (m_n R) \left(m_n^2 I_0 (m_n r_0)\right.$$
$$\left. - \beta m_n I_1 (m_n r_0)\right) - I_0 (m_n R) \left(m_n^2 K_0 (m_n r_0) + \beta m_n K_1 (m_n r_0)\right)\Big) \tag{A20}$$

In order to find the values of s that make Eq. A18 zero, it is useful to make the following substitution:

$$\frac{s}{a} + m_n^2 = -\alpha_n^2$$

This gives

$$\Delta = K_0 (i\alpha_n R) \left(\left(\frac{-a \left(\alpha_n^2 + m_n^2\right)}{a_w} + m_n^2 \right) I_0 (i\alpha_n r_0) - \beta i \alpha_n I_1 (i\alpha_n r_0) \right)$$
$$- I_0 (i\alpha_n R) \left(\left(\frac{-a \left(\alpha_n^2 + m_n^2\right)}{a_w} + m_n^2 \right) K_0 (i\alpha_n r_0) + \beta i \alpha_n K_1 (i\alpha_n r_0) \right) \tag{A21}$$

In order to simplify Eq. A21, we make use of the following identities (e.g., Ref. [12], Appendix III).

$$I_0 (ix) = J_0 (x) \quad I_1 (ix) = i J_1 (x) \quad K_0 (ix) = (\pi i/2) \left(-J_0 (x) + i Y_0 (x)\right)$$

$$K_1 (ix) = (\pi/2) \left(-J_1 (x) + i Y_1 (x)\right)$$

This gives

$$\Delta = \frac{\pi}{2} J_0(\alpha_n R)\left(\left(\frac{-a\left(\alpha_n^2+m_n^2\right)}{a_w}+m_n^2\right)Y_0(\alpha_n r_0)+\beta\alpha_n Y_1(\alpha_n r_0)\right) - \frac{\pi}{2} Y_0(\alpha_n R)\left(\left(\frac{-a\left(\alpha_n^2+m_n^2\right)}{a_w}+m_n^2\right)J_0(\alpha_n r_0)+\beta\alpha_n J_1(\alpha_n r_0)\right) \quad \text{(A22)}$$

Equation A22 is an even function with respect to real α_n. It is cyclic and has roots along the real axis. For the jth positive real root ($\alpha_{j,n}$), the residue is given by

$$\operatorname{res}\left(s=-a\left(\alpha_{j,n}^2+m_n^2\right)\right)=\frac{b_n e^{-a\left(\alpha_{j,n}^2+m_n^2\right)t}}{-a\left(\alpha_{j,n}^2+m_n^2\right)\frac{d\Delta}{ds}|_{s=-a\left(\alpha_{j,n}^2+m_n^2\right)}}\Phi\left(\alpha_{j,n}\right) \quad \text{(A23)}$$

where

$$\begin{aligned}\Phi\left(\alpha_{j,n}\right) &= \left(K_0\left(i\alpha_{j,n}R\right)I_0\left(i\alpha_{j,n}r\right)-I_0\left(i\alpha_{j,n}R\right)K_0\left(i\alpha_{j,n}r\right)\right)\\ &= (\pi/2)\left(J_0\left(\alpha_{j,n}R\right)Y_0\left(\alpha_{j,n}r\right)-Y_0\left(\alpha_{j,n}R\right)J_0\left(\alpha_{j,n}r\right)\right)\end{aligned} \quad \text{(A24)}$$

Differentiating Eq. A22 with respect to s gives

$$\begin{aligned}\frac{d\Delta}{ds} = \frac{-\pi}{4a\alpha_n}\{&-RJ_1(\alpha_n R)\left[A_n Y_0(\alpha_n r_0)+\beta\alpha_n Y_1(\alpha_n r_0)\right]\\ &+J_0(\alpha_n R)\left[\left(\beta\alpha_n r_0-2\alpha_n\left(a/a_w\right)\right)Y_0(\alpha_n r_0)-A_n r_0 Y_1(\alpha_n r_0)\right]\\ &+RY_1(\alpha_n R)\left[A_n J_0(\alpha_n r_0)+\beta\alpha_n J_1(\alpha_n r_0)\right]\\ &-Y_0(\alpha_n R)\left[\left(\beta\alpha_n r_0-2\alpha_n\left(a/a_w\right)\right)J_0(\alpha_n r_0)-A_n r_0 J_1(\alpha_n r_0)\right]\}\end{aligned} \quad \text{(A25)}$$

where

$$A_n = \frac{-a\left(\alpha_n^2+m_n^2\right)}{a_w}+m_n^2$$

Most or all of the roots of Eq. A22 (with $\Delta = 0$) fall on the real axis, and thus Eqs. A23 and A24 are convenient for evaluating the residues. However, for certain circumstances two roots ($\alpha_n = \pm i\phi_n$) also appear on the imaginary axis for Eq. A22 (corresponding to a single pole on the negative real axis for s in Eq. A17). If these roots are recovered, then, in principle, Eq. A23 can also be used to evaluate the residue. However, since it is more convenient to avoid the use of complex numbers in the final evaluation, it is better to make the following substitution in Eq. A18:

$$\frac{s}{a}+m_n^2=\phi_n^2 \quad \text{(A26)}$$

Therefore, we have

$$\Delta = K_0(\phi_n R)\left(\left(\frac{a\left(\phi_n^2 - m_n^2\right)}{a_w} + m_n^2\right) I_0(\phi_n r_0) - \beta\phi_n I_1(\phi_n r_0)\right) - I_0(\phi_n R)\left(\left(\frac{a\left(\phi_n^2 - m_n^2\right)}{a_w} + m_n^2\right) K_0(\phi_n r_0) + \beta\phi_n K_1(\phi_n r_0)\right) \tag{A27}$$

The residue for the pole corresponding to the value of ϕ_n that makes Eq. A27 zero is given by

$$\operatorname{res}\left(s = a\left(\phi_n^2 - m_n^2\right)\right) = \frac{be^{-a\left(m_n^2-\phi_n^2\right)t}}{a\left(\phi_n^2 - m_n^2\right)\frac{d\Delta}{ds}|_{s=a\left(\phi_n^2-m_n^2\right)}} \quad (K_0(\phi_n R) I_0(\phi_n r) - I_0(\phi_n R) K_0(\phi_n r)) \tag{A28}$$

The derivative of Eq. (A27) with respect to s is given by

$$\begin{aligned}\frac{d\Delta}{ds} = \frac{1}{2\phi_n a}[&(K_0(\phi_n R) I_0(\phi_n r_0) - I_0(\phi_n R) K_0(\phi_n r_0))(2(a/a_w) - \beta r_0)\phi_n \\ &+ (r_0 K_0(\phi_n R) I_1(\phi_n r_0) - R K_1(\phi_n R) I_0(\phi_n r_0)) B_n \\ &+ (r_0 I_0(\phi_n R) K_1(\phi_n r_0) - R I_1(\phi_n R) K_0(\phi_n r_0)) B_n \\ &+ (K_1(\phi_n R) I_1(\phi_n r_0) - I_1(\phi_n R) K_1(\phi_n r_0))\beta\phi_n R]\end{aligned} \tag{A29}$$

where

$$B_n = m_n^2 + \frac{\left(\phi_n^2 - m_n^2\right)a}{a_w}$$

The derivation is almost complete. In order to obtain the final result given in Eq. 8, the residues specified by Eqs. A20, A23, and A28 are summed over all j for each value of n. Finally, the inverse finite Fourier transform specified in Eq. A8 is applied. Note that in Eq. 8, θ_n includes only the transient parts of the solution (for clarity), while in this appendix it includes both transient and steady parts.

Appendix B

Conditions for Which Eq. 17 has Real Roots

The term $\zeta_n(\phi_n)$ in Eq. 12 only appears if Eq. 17 has real roots. Therefore, it is necessary to clarify the conditions at which this occurs. We wish to verify the following conditions already noted in Eqs. 15 and 16.

1. Equation 17 does not have a positive real root if $a_w > a$

2. Equation 17 has a positive real root if and only if $m_n^2 > \beta/\{((a/a_w) - 1)\, r_0 \ln(R/r_0)\}$

Note that since Eq. 17 can be derived by substituting $\alpha_n = \mathrm{i}\,\phi_n$ in Eq. 13, where ϕ_n is a real number, then the existence of real roots for Eq. 17 also implies the existence of complex roots (on the imaginary axis) in Eq. 13. Let $W(\phi_n)$ denote the expression on the left-hand side of Eq. 17. Therefore, we may write

$$W(\phi_n) = (I_0(\phi_n R)\, K_0(\phi_n r_0) - K_0(\phi_n R)\, I_0(\phi_n r_0)) \left(\left(\phi_n^2 - m_n^2\right)(a/a_w) + m_n^2\right) + (I_0(\phi_n R)\, K_1(\phi_n r_0) + K_0(\phi_n R)\, I_1(\phi_n r_0))\, \beta\phi_n = 0 \tag{B1}$$

For real ϕ_n, $W(\phi_n)$ is an even function. This may be verified by substituting $-\phi_n$ for ϕ_n and making use of the following identities:

$$I_0(-x) = I_0(x), \quad I_1(-x) = -I_1(x), \quad K_0(-x) = -\pi i I_0(x) + K_0(x)$$

$$K_1(-x) = -\pi i I_1(x) - K_1(x)$$

Therefore, if ϕ_n is a positive real root of Eq. 17, then $-\phi_n$ is also a root. Since based on Eq. A25 we are only interested in ϕ_n^2, it is sufficient to consider only the positive root.

The modified Bessel functions, $I_0(x)$, $K_0(x)$, $I_1(x)$, and $K_1(x)$, are positive for all positive real values of x. Therefore, the term $(I_0(\phi_n R)\, K_1(\phi_n r_0) + K_0(\phi_n R)\, I_1(\phi_n r_0))\beta\phi_n$ in Eq. B1 is positive for positive ϕ_n since r and R are also positive real numbers. Note also that for $R > r_0$ the following inequalities are also true since $I_0(x)$ increases monotonically with increasing x and $\mathrm{K}_0(x)$ decreases monotonically with increasing x:

$$I_0(\phi_n R) > I_0(\phi_n r)$$

$$K_0(\phi_n R) < K_0(\phi_n r)$$

Therefore,

$$I_0(\phi_n R)\, K_0(\phi_n r) > K_0(\phi_n R)\, I_0(\phi_n r)$$

Thus, the factor $(I_0(\phi_n R)\, K_0(\phi_n r_0) - K_0(\phi_n R)\, I_0(\phi_n r_0))$ in Eq. B1 is also positive. Therefore, the only way that $W(\phi_n)$ can be zero is if

$$\left(\phi_n^2 - m_n^2\right)(a/a_w) + m_n^2 < 0 \tag{B2}$$

Rearranging Eq. B2, we obtain

$$\phi_n^2 < m_n^2 \left(1 - \frac{a_w}{a}\right) \tag{B3}$$

Therefore, since m_n^2 is a positive number and Eq. B3 cannot be satisfied if the right-hand side is negative, no positive real root to Eq. 17 can exist if the thermal diffusivity of the wire, a_w is greater than the thermal diffusivity of the gas, a. Thus, statement 1 at the beginning of this appendix is verified. Also, Eq. 19 follows from Eq. B3.

In order to verify statement 2, first we rewrite Eq. B1 in the following form:

$$W(\phi_n) = W_1(\phi_n) W_2(\phi_n) + \beta W_3(\phi_n) \tag{B4}$$

where

$$W_1(\phi_n) = (I_0(\phi_n R) K_0(\phi_n r_0) - K_0(\phi_n R) I_0(\phi_n r_0)) \tag{B5}$$

$$W_2(\phi_n) = \left(\left(\phi_n^2 - m_n^2\right)(a/a_w) + m_n^2\right) \tag{B6}$$

$$W_3(\phi_n) = (I_0(\phi_n R) K_1(\phi_n r_0) + K_0(\phi_n R) I_1(\phi_n r_0))\phi_n \tag{B7}$$

It is possible to verify that Eqs. B5–B7 increase monotonically with increasing positive real values of ϕ_n for $R > r_0$. Therefore, the function $W(\phi_n)$ given in Eq. B4 also increases monotonically for increasing positive ϕ_n. This property of the function $W(\phi_n)$ implies that there can be only one positive real root to Eq. B1. Since for large values of ϕ_n, $W(\phi_n)$ is positive; if the root exists, then the following inequality must be true:

$$\lim_{\phi_n \to 0} W(\phi_n) < 0 \tag{B8}$$

Making use of the expansions in Ref. [15] it can be shown that

$$\lim_{\phi_n \to 0} W(\phi_n) = m_n^2 (1 - (a/a_w)) \ln(R/r_0) + (\beta/r_0) \tag{B9}$$

Substituting Eq. B9 into B8 and rearranging gives

$$m_n^2 > \frac{\beta}{((a/a_w) - 1) r_0 \ln(R/r_0)} \tag{B10}$$

Thus, Eq. B10 is the necessary condition for the existence of a real positive root to Eq. 17.

References

1. M. Fujii, X. Zhang, N. Imaishi, S. Fujiwara, T. Sakamoto, Int. J. Thermophys. **18**, 327 (1997)
2. X. Zhang, S. Fujiwara, Z. Qi, M. Fujii, J. Jpn. Soc. Micrograv. Appl. **16**, 129 (1999)
3. X. Zhang, W. Hendro, M. Fujii, T. Tomimura, N. Imaishi, Int. J. Thermophys. **23**, 1077 (2002)
4. N. Sakoda, E. Yusibani, P.L. Woodfield, K. Shinzato, M. Kohno, Y. Takata, M. Fujii, in *Proceedings 8th Asian Thermophysical Properties*. Conference, Fukuoka, Japan (August 2007)
5. P.L. Woodfield, J. Fukai, M. Fujii, Y. Takata, K. Shinzato, Int. J. Thermophys., doi:10.1007/s10765-008-0468-z
6. M.J. Assael, L. Karagiannidis, N. Malamataris, W.A. Wakeham, Int. J. Thermophys. **19**, 379 (1998)
7. J.J. Healy, J.J. de Groot, J. Kestin, Physica **82C**, 392 (1976)
8. M.J. Assael, C.A. Nieto de Castro, H.M. Roder, W.A. Wakeham, in *Experimental Thermodynamics, Vol. III, Measurement of the Transport Properties of Fluids*, IUPAC Chemical Data Series, No. 37, ed. by W.A. Wakeham, A. Nagashima, J.V. Sengers (Blackwell Scientific Publications, Great Britain, 1991), p. 163
9. W.T. Kierkus, N. Mani, J.E.S. Venart, Can. J. Phys. **51**, 1182 (1973)
10. W.G. Kannuluik, L.H. Martin, Proc. Royal Soc. Lond. A, **144**, 496 (1934)
11. W.G. Kannuluik, Proc. Royal Soc. Lond. A **131**, 320 (1931)
12. H.S. Carslaw, J.C. Jaeger, *Conduction of Heat in Solids*, 2nd edn. (Oxford University Press, Great Britain, 2003)
13. J.C. Jaeger, J. Proc. Royal Soc. New South Wales **74**, 342 (1940)
14. J.C. Jaeger, J. Proc. Royal Soc. New South Wales **75**, 130 (1942)
15. M. Abramowitz, I.A. Stegun (eds.), *Handbook of Mathematical Functions: With Formulas, Graphs and Mathematical Tables* (Dover, New York, 1972)
16. S. Kakac, Y. Yener, *Heat Conduction*, 2nd edn. (Hemisphere, New York, 1985), pp. 244–276